EFFECT OF INCREASING RCS ON SPACE OBJECT DETECTABILITY FROM A NETWORK OF EUROPEAN SPACE DEBRIS MONITORING SENSORS

Alexandru Mancas[1], Tim Flohrer[2], Stijn Lemmens[2]

[1] GMV Insyen/ESOC, Robert-Bosch-Str. 5, Darmstadt, Germany, Email: alexandru.mancas@esa.int
[2] European Space Agency, Robert-Bosch-Str. 5, Darmstadt, Germany, Email: tim.flohrer@esa.int, stijn.lemmens@esa.int

ABSTRACT

ESA's SSA programme aims to act as architects of a system of European Space Debris Monitoring (SDmon) systems and ESA has developed an end-to-end SDmon architecture simulation tool. The need for timely and accurate SDmon data is increasing, driven by the recent launches of massive numbers of small satellites and the announcements of several large constellations.

Increasing the radar cross-section (RCS) of targets with retroreflectors can improve the coverage of SDmon sensors. The paper investigates how the increase of observability parameters can affect the coverage and orbit maintenance from a hypothetical future European SDmon system.

A complete network consisting of existing European sensors and test targets with different cross-sections, but the same orbits, were simulated. Targets placed in representative orbits for small satellites had their cross-section varied between 0.1 m^2 and 10 m^2.

The results show increased cross-section providing a small, but significant, improvement especially in detectability, initial acquisition, and the covariance of the catalogued orbit.

Adding retro-reflectors to increase the RCS is not a game-changer, but it can provide benefits at critical moments, especially when the satellite is first detected. The results depend strongly on the sensor architecture chosen, so more work is needed to simulate 'realistic' SDmon systems.

1 INTRODUCTION

The ESA Space Safety/Space Situational Awareness (SSA) programme contains activities for space weather, near-Earth objects, and space debris monitoring. International partners include COSPAR, IADC (Inter-Agency Space Debris Coordination Committee), UN COPUOS (United Nations Committee on the Peaceful Uses of Outer Space), and ESO (European Southern Observatory) [1]. The Space Debris Office's expertise includes collision avoidance support, re-entry risk assessment, and the development of space debris environment models [2].

ESA has recently (2015-2018) run a project that aimed to develop an end-to-end SDmon system architecture simulation tool, named SSATAN. The tool can estimate the performance of a variety of sensor architectures (radars, ground and space-based telescopes) with various space object populations.

Over the past two decades there has been a boom in CubeSat launches; multiple launch service providers have more than 100 launches since 2011, and 10 more are scheduled to start offering launch services in 2019 [3]. The small size and typical lack of a propulsion system can pose an increased risk of collision with other operational spacecraft.

This paper aims to investigate if increasing the radar cross-section (RCS) of CubeSats (eg by adding retroreflectors) can produce any meaningful benefits to detectability and cataloguing.

2 SIMULATION SET-UP

The approach used was to define a space object population in representative low Earth orbits for current CubeSats, multiple objects in the same orbit with different RCSs, and a network of small SDmon radars located in Europe.

2.1 SSATAN

The Space Surveillance ArchiTecture ANalysis tool (SSATAN) is a modular simulator of SDmon architectures. It consists of the following modules, which are run in a sequential manner [4]:

- Population generation: allows the generation of a population of space objects, based on TLE and MASTER data, and the insertion of fragmentations or re-entering objects;
- Measurement generation: allows the definition of a network of sensors (including performance parameters and location), propagates the population generated in the previous step and generates synthetic measurements;
- Cataloguing: generates a catalogue of objects from the observations and the sensor architecture; includes correlation, preliminary

orbit determination, sequential orbit determination, propagation, etc; simulators are available for some steps (correlation and preliminary orbit determination);
- Analysis tools: provide some information on the outputs of the other modules.

SSATAN is currently being tested and ESA is investigating improvements, including better sensor performance models and improved performance.

2.2 Space objects used in the simulations

Six orbits were chosen for the space object population, and four RCS values were used for each orbit, leading to 64 total objects. Six common orbits for CubeSats were chosen [3] and are listed in Tab. 1. As TLEs were used as input for population generation, 6 objects, not all of them CubeSats, one in each orbit, were used to generate the population.

Table 1- Orbital parameters for the simulated objects

"archetype"	altitude [km]	inclination [°]
SENSE SV2	369	40.5
SENTINEL 2B	789	98.5
EAGLESAT 1	639	97.7
TINTIN A	510	97.4
COSMOS 2525	280	96.6
AEROCUBE 12B	488	51.6

For each orbit, three object diameters were used: 30 cm, 50 cm, 1 m, and 10 m. All the objects in one orbit had the same ballistic coefficient, to ensure the orbit stays consistent over the entire simulation timespan.

2.3 Radars used in the simulation

A system composed of two small hypothetical tracking/surveillance radars was chosen for the simulation. The two hypothetical radars were chosen to approximate the estimated performance of the Spanish and German Space Surveillance radars [5,6].

An overview of the parameters used can be seen in Tab. 2. Both simulated radars were set to detect 1 m^2 objects at 1000 km with an SNR of 13 dB, to need an SNR of 9 dB to detect an object, have a 20 m 1-way range accuracy and produce observations every 5 s. SSATAN was set to generate observations whenever the target was in the field-of-regard (FoR) and detectable.

Table 2 - Parameters for the simulated radars

parameter	radar 1	radar 2
location	southern Spain	north-western Germany
reference RCS [m^2]	1.0	1.0
reference distance [km]	1000.0	1000.0
reference SNR [dB]	13.0	13.0
minimum SNR for detection [dB]	9.0	9.0
azimuth range [°]	90-270	0-360
elevation range [°]	30-80	30-90
maximum detection range [km]	8000.0	8000.0
range accuracy [m]	20	20
observation frequency [s]	5.0	5.0

The performance of the radars will play a large part in the results. The radar parameters and range of target diameters were chosen to be realistic, but at the same time show some differences in the results. For example, if two radars capable of detecting 1 cm objects at 5000 km were used, all targets in one orbit would show the same results.

2.4 Other simulation parameters

Other parameters used in the simulation were:

- 10 day total duration;
- Catalogue cold start;
- 15 minute timestep for cataloguing.

3 RESULTS

Two aspects of the results were analysed: observability (the synthetic measurements produced by the SSATAN measurement generation module) and cataloguing accuracy, ie the post-orbit determination (OD) covariance of the catalogued objects.

3.1 Observability

The number of tracks and average track duration for all radar/target pairs can be seen in Tab. 3. The general trend is the larger the targets, the higher the number of tracks and the longer the individual tracks. There is a point of diminishing returns, and at some diameter the target is observable whenever it is in the radar's FoR. This effect is visible in the 280 km x 96.6° targets, where the 1 m and 10 m diameter targets have the same tracks, and the drop-off to 50 cm is small.

The two radars generally do not observe the smaller (30 cm and 50 cm) objects, or generate fewer tracks for them, even for some of the lower altitude objects. For example, for the 789 km objects, no tracks of the smaller objects are generated, while for the 639 km objects only 3 tracks are generated for the 50 cm object.

Table 3 - Number of tracks and average track duration for all radar/target pairs

radar-1		radar-2			target properties		
tracks	**average duration [s]**	**tracks**	**average duration [s]**	**total tracks**	**diameter [m]**	**altitude [km]**	**inclination [°]**
21	52	0	n/a	21	0.3	369	40.5
27	72	0	n/a	27	0.5		
33	76	0	n/a	33	1		
34	80	0	n/a	34	10		
0	n/a	0	n/a	0	0.3	789	98.5
0	n/a	0	n/a	0	0.5		
7	75	9	119	16	1		
20	179	27	171	47	10		
0	n/a	0	n/a	0	0.3	639	97.7
2	48	1	40	3	0.5		
9	97	8	118	17	1		
19	171	27	169	46	10		
2	33	1	30	3	0.3	510	97.4
6	59	10	42	16	0.5		
11	103	18	87	29	1		
14	111	20	109	34	10		
1	45	10	51	11	0.3	280	96.6
4	44	10	64	14	0.5		
5	45	10	70	15	1		
5	45	10	70	15	10		
4	63	12	51	16	0.3	488	51.6
7	109	20	99	27	0.5		
17	123	29	142	46	1		
21	129	34	151	55	10		

3.2 Cataloguing

The analysis of the cataloguing performance focuses on the post-sequential orbit determination covariance, as this can drive the probability of collision for any close conjunctions.

3.2.1 369 km x 40.5°

Objects in the 369 km x 40.5° orbits were detected only by the radar in southern Spain, due to their low inclination. A plot of along-track position σ against simulation time for the first 5 days of the simulation can be seen in Fig. 1. All four objects are detected in first day, and the σ decreases with increasing object size. This difference is large in the first few OD runs, but decreases with time, from 30+ m to a few m.

The difference in the number of tracks is not that large, so the OD is run at about the same frequency, but due to the longer tracks the post-OD covariance is smaller for the larger objects.

3.2.2 789 km x 98.5°

Only the larger two objects (1 m and 10 m) in the 789 km x 98.5° orbits were detected and catalogued, due to the higher altitude. A plot of along-track position σ against simulation time for the first 5 days of the simulation can be seen in Fig. 2. The 10 m object is catalogued in the first day, while the 1 m object is catalogued at the end of the second day.

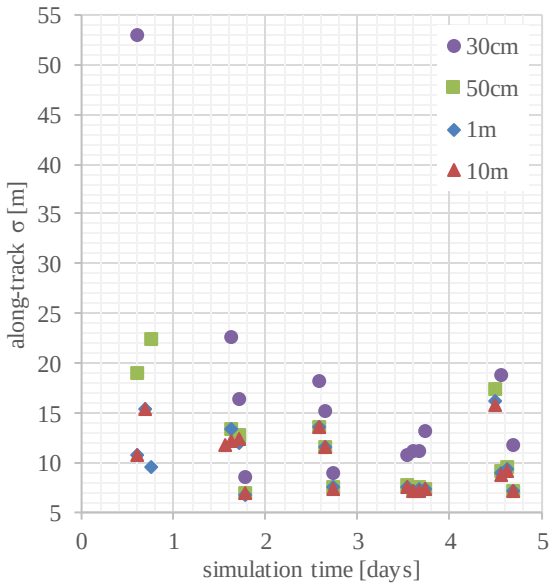

Figure 1 - Along-track position σ for 369 km altitude, 40.5° inclination objects

The 10 m object has more tracks and therefore more frequent OD runs. Due to the longer and more frequent tracks the post-OD covariance is smaller for the larger object and the two do not seem to converge to the same value.

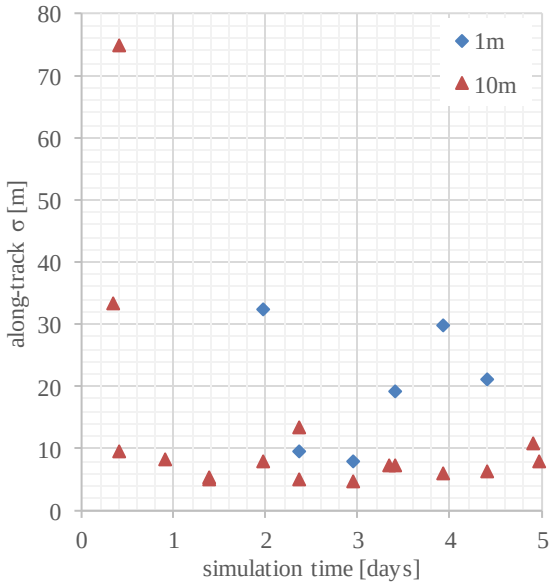

Figure 2 - Along track position σ for 789 km altitude, 98.5° inclination

There is one point (at ≈ 2.4 days) where there are two OD runs for the 10 m object in successive timesteps and one run for the 1 m object only in the latter timestep where the reverse appears to be true. However, the 10 m object has the smaller covariance in the same timestep, but a larger one in the previous timestep, when the 1 m object was not observed.

3.2.3 639 km x 97.7°

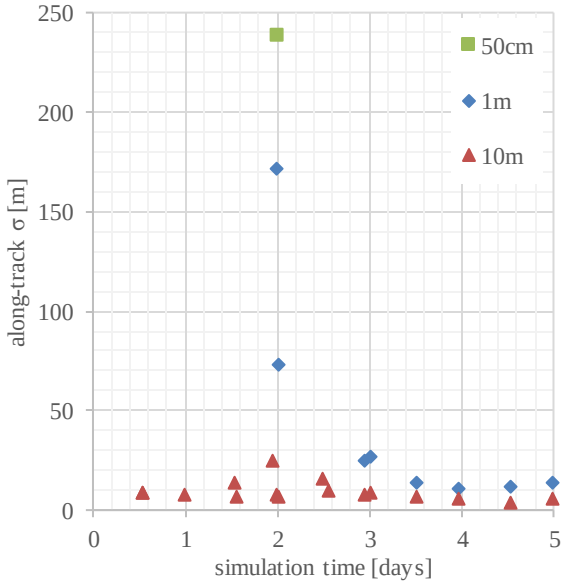

Figure 3 - Along-track position σ for 639 km altitude, 97.7° inclination

The 639 km x 97.7° case has some similarities to 789 km x 98.5°. The along-track position σ plot can be seen in Fig. 3. The 50 cm object is only observed 3 times in 10 days. In the first 5 days there is only one OD run, but the along-track position σ is above the accuracy envelope of the catalogue (200 m), so the object is not catalogued. The 1m object is detected after 2 days, and while its along-track position σ start high, it becomes very close to the 10 m object after 2 days.

3.2.4 510 km x 97.4°

The 510 km x 97.4° case (along-track position σ plot in Fig. 4) shows some similarities to 639 km x 97.7° and 789 km x 98.5°. The 30 cm object is only observed 3 times in 10 days. In the first 5 days there is only one OD run, but the along-track position σ is above the accuracy envelope of the catalogue (200 m), so the object is not catalogued. The 50cm, 1m, and 10 m object are detected in the first day. The along-track position σ of the 50 cm object starts high, but it comes very close to the other objects after 1.5 days before increasing a bit again. The 1 m and 10 m objects have very similar σ after 1.5 days.

3.2.5 280 km x 96.6°

The 280 km x 96.6 ° case did not lead to any reliable OD results. There were 2 OD runs for the 30 cm object, with 1 km along-track sigma after the second, and only one for each of the 50 cm , 1m, and 10 m objects.

It is not clear what lead to the sparse OD, as each object had at least 10 tracks from one of the radars.

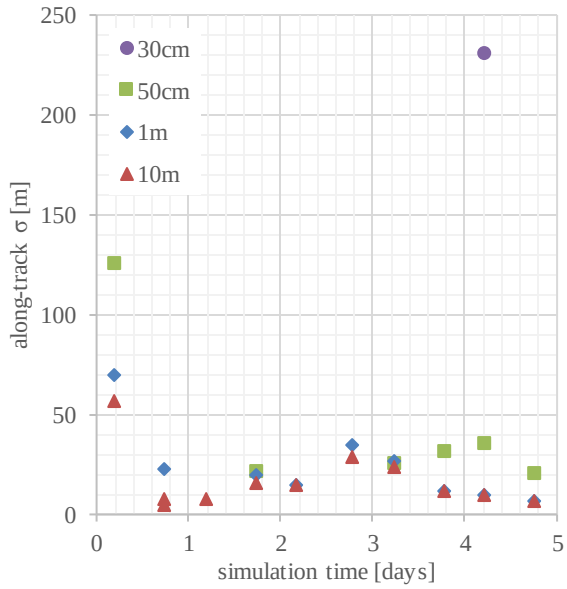

Figure 4 - Along track position σ for 510 km altitude, 97.4° inclination

3.2.6 488 km x 51.5°

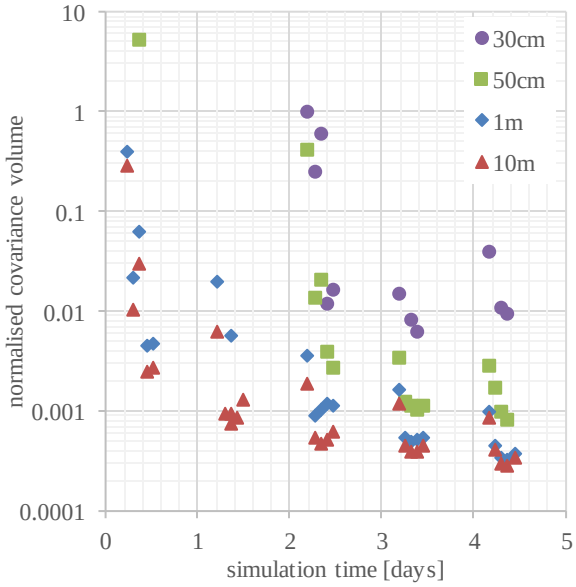

Figure 5 - Normalised position covariance volume (earliest covariance of the smallest object is 1) for 488 km altitude and 51.5° inclination

Fig. 5 shows the normalised position covariance ellipsoid volumes on a log plot for the 488 km x 51.5° case. The first position covariance ellipsoid of the 30 cm object has a volume of 1. This plot shows the differences between different diameter objects better, but removes some of the quantitative meaning.

The 1 m, and 10 m objects are all detected in the first day and have similar covariance, with the 10 m object slightly smaller. The 30 and 50 cm object are not detected until the third day and have larger covariance than the other objects, with the 30 cm having a larger covariance than the 50 cm object. The 50 cm has one OD run in the first day, but the covariance was too high to keep it catalogued.

4 SUMMARY AND CONCLUSIONS

The effect of increasing the RCS of CubeSats on improving detectability and cataloguing has been investigated. For the test cases considered (typical CubeSat LEO orbits, two small radars in Europe), increasing the RCS leads to better observability, faster cataloguing, and smaller position covariance.

The 10 m diameter objects were catalogued in the first day for all orbital regimes, and the same applies to the 1 m objects in all but the highest altitude (789 km) orbit. The larger objects have smaller covariance, but there are two points of diminishing returns:

- at some object size for an orbit/radar pair, the object is detectable for the entire pass; increasing size will not improve detectability or reduce covariance; this is the case for the 1 m and 10 m objects at 369 km x 40.5°;
- given enough passes (ie more time since the first cataloguing), the covariance trends to similar values; this is the case for the 1 m and 10 m objects at 639 km x 97.7°.

These first results show that increasing RCS is beneficial for cataloguing space objects, but more work is needed simulating actual architectures and improving the related sensor performance models.

5 REFERENCES

1. "SSA Programme overview". ESA website. https://www.esa.int/Our_Activities/Operations/Space_Situational_Awareness/SSA_Programme_overview
2. " Space Debris Office ". ESA website. https://www.esa.int/Our_Activities/Operations/gse/ESA_Space_Debris_Office
3. "Nanosats database". nanosats.eu
4. "SST Analysis Tool Algorithms Document". Issue 2. Revision 3. European Space Agency, April 2018.
5. Gómez, Inés Alonso, Sara Ansorena Vildarraz, Carlos García, María Antonia Ramos Prada, Juan Ureña Carazo, Gian Maria Pinna, Serge Moulin et al. "Description of the Architecture of the Spanish Space Surveillance and Tracking System." In Proceedings of the 7th European Conference on Space Debris. 2017.
6. Wilden, H., C. Kirchner, O. Peters, N. Ben Bekhti, R. Kohlleppel, A. Brenner, and T. Eversberg. "GESTRA - technology aspects and mode design for space surveillance and tracking." In Proceedings of the 7th

European Conference on Space Debris, Darmstadt, Germany, pp. 18-21. 2017.